Automatica 45 (2009) 405–415

Contents lists available at ScienceDirect

Automatica

journal homepage: www.elsevier.com/locate/automatica

Control of mechanical motion systems with non-collocation of actuation and friction: A Popov criterion approach for input-to-state stability and set-valued nonlinearities[☆]

J.C.A. de Bruin[a], A. Doris[b,1], N. van de Wouw[a,*], W.P.M.H. Heemels[a], H. Nijmeijer[a]

[a] Eindhoven University of Technology, Department of Mechanical Engineering, P.O. Box 513, NL 5600 MB Eindhoven, The Netherlands

[b] Shell International Exploration and Production B.V., Keslerpark 1, 2288 GS Rijswijk, The Netherlands

ARTICLE INFO

Article history:
Received 23 August 2007
Received in revised form
14 May 2008
Accepted 11 September 2008
Available online 27 December 2008

Keywords:
Motion control
Absolute stability
Discontinuous systems
Friction
Output-feedback control
Stabilisation

ABSTRACT

The presence of friction in mechanical motion systems is a performance limiting factor as it induces stick–slip vibrations. To appropriately describe the stiction effect of friction, we adopt set-valued force laws. Then, the complete motion control system can be described by a Lur'e system with set-valued nonlinearities. In order to eliminate stick–slip vibrations for mechanical motion systems, a state-feedback control design is presented to stabilize the equilibrium. The proposed control design is based on an extension of a Popov-like criterion to systems with set-valued nonlinearities that guarantees input-to-state stability (ISS). The advantages of the presented controller is that it is robust to uncertainties in the friction and it is applicable to systems with non-collocation of actuation and friction where common control strategies such as direct friction compensation fail. Moreover, an observer-based output-feedback design is proposed for the case that not all the state variables are measured. The effectiveness of the proposed output-feedback control design is shown both in simulations and experiments for a typical motion control system.

1. Introduction

In many mechanical motion systems, the presence of friction gives rise to undesired behavior such as steady-state positioning errors, large settling times and stick–slip vibrations (Armstrong-Hélouvry, 1991; Armstrong-Hélouvry, Dupont, & Canudas de Wit, 1994; Canudas de Wit, Olsson, Åström, & Lischinsky, 1995; Olsson, Åström, Canudas de Wit, Gafvert, & Lischinsky, 1998). Especially, friction-induced stick–slip vibrations lead to kinetic energy dissipation, noise, excessive wear, premature failure of machine parts and inferior positioning performance. Research on the presence of friction-induced stick–slip vibrations is conducted for different mechanical systems; e.g. drilling systems (Jansen & van den Steen, 1995; Navarro-López & Suárez, 2004), flexible rotor systems (Mihajlović, van de Wouw, Hendriks, & Nijmeijer, 2006; Mihajlović, van Veggel, van de Wouw, & Nijmeijer, 2004), robots (Jeon & Tomizuka, 2005), servo systems (Olsson & Åström, 2001), turbine blade dampers (Pfeiffer & Hajek, 1992), etc. In this paper, a control strategy for mechanical motion systems is proposed in order to eliminate the undesired friction-induced stick–slip vibrations and to guarantee stability of the desired setpoint. The proposed control strategy is applied to an experimental setup and its effectiveness is shown in experiments. To properly describe the stiction effect in dry friction, set-valued friction models are commonly used (Brogliato, 2004; Glocker, 2001; Leine & Nijmeijer, 2004), which lead to dynamic models in terms of differential inclusions (Aubin & Cellina, 1984; Brézis, 1973; Filippov, 1988).

A common approach to tackle motion control problems for systems with (set-valued) friction is the application of direct friction compensation techniques, see e.g. (Armstrong-Hélouvry, 1991; Armstrong-Hélouvry et al., 1994; Olsson et al., 1998; Putra, van de Wouw, & Nijmeijer, 2007; Southward, Radcliffe, & MacCluer, 1991; Swevers, Al-Bender, Ganseman, & Projogo, 2000) and many others. Since friction characteristics are known to be sensitive to temperature, humidity, etc., it may be hard to obtain accurate friction models with limited complexity suitable

☆ Supported by European project SICONOS (IST-2001-37172) and by the Netherlands Organisation for Scientific Research (NWO). This paper was recommeded for publication in revised form by Associate Editor Yoshikazu Hayakawa under the direction of Editor Toshiharu Sugie. The material in this paper was partially presented at A part is presented at 3rd IFAC Workshop 'Periodic Control Systems' 29–31 August 2007, St Petersburg.

* Corresponding author. Tel.: +31 40 247 3358; fax: +31 40 246 1418.
E-mail addresses: jcadebruin@gmail.com (J.C.A. de Bruin), Apostolos.Doris@shell.com (A. Doris), N.v.d.Wouw@tue.nl (N. van de Wouw), W.P.M.H.Heemels@tue.nl (W.P.M.H. Heemels), H.Nijmeijer@tue.nl (H. Nijmeijer).

1 This work was performed while affiliated with the Eindhoven University of Technology.

0005-1098/$ – see front matter © 2008 Elsevier Ltd. All rights reserved.
doi:10.1016/j.automatica.2008.09.008

for a compensation scheme. Furthermore, the absence of accurate friction models has been shown to be a performance limiting factor in employing friction compensation in practice (Canudas de Wit, 1993; Mallon, van de Wouw, Putra, & Nijmeijer, 2006), leading to limit cycles and steady-state errors. This indicates a first drawback of a typical compensation technique that it is not robust to friction uncertainties. Moreover, common friction compensation schemes are typically applied when the actuation and friction are collocated, meaning that the friction force and the actuation force act at the same place and the friction can be compensated directly (if an accurate friction model is available). However, this is not the case for many mechanical systems. Here, we are interested in a feedback control approach for motion systems with non-collocation of actuation and friction, that is inherently robust to uncertainties in the friction characteristic.

A robust compensation approach is discussed in Taware, Tao, Pradhan, and Teolis (2003), where they consider a motor-load system with, possibly discontinuous, friction at the load and joint flexibility and damping (between the motor and the load). However, the model reference adaptive control scheme does not guarantee a zero tracking error. A variable structure control design is presented in Kwatny, Teolis, and Mattice (2002) for systems with nonsmooth uncertainties, where the intended application is for systems in which the uncertain friction forces are relatively small. Since for motion systems exhibiting friction-induced vibrations the friction forces are relatively large, the latter approach is not directly applicable. Another approach for controller design can be based on the well-known absolute stability theory, using circle or Popov criteria (see e.g. Khalil (2002)). In particular, stabilization techniques based on absolute stability theory for locally Lipschitzian systems with slope-restricted nonlinearities are discussed in Arcak and Kokotović (2001) and Arcak, Larsen, and Kokotović (2003), which are not applicable to the systems under study since they contain set-valued nonlinearities to accurately describe the friction. A generalized circle criterion, that is suitable for systems with set-valued nonlinearities, is discussed in Brogliato (2004). Unfortunately, the conditions of the circle criterion are rather restrictive for typical motion control applications as will be indicated in this paper.

In this paper, we present a generalization of the Popov-like criterion, in the sense that it is applicable to systems with set-valued nonlinearities. Moreover, we obtain input-to-state stability (ISS) (instead of only asymptotic stability) with respect to perturbations on the system (e.g. measurement noise). In analogy with the "absolute stability" property, obtained by satisfaction of the conventional Popov-criterion, one might call this property "absolute ISS". The concept of absolute ISS is used for the design of a state-feedback controller for mechanical motion systems with set-valued nonlinearities that can be described by Lur'e-type systems, i.e. linear systems with set-valued nonlinearities in the feedback loop. An advantage of the proposed control design is that it is applicable to systems with non-collocation of actuation and set-valued friction laws, a situation that has not been studied in literature before, at least not in the generality as presented here. Moreover, the fact that the satisfaction of such an adapted Popov criterion guarantees absolute ISS implies robustness with respect to uncertainties in the friction and measurement errors. Next, the ISS property is used to construct an observer-based output-feedback controller cf. Doris et al. (2008). Finally, we provide a separation principle for the output-feedback controlled system, i.e. the controller and the observer can be designed separately.

The notion of ISS (Sontag, 1989) is a useful property in the field of control, which ensures that the state of the system is bounded for a bounded input. In Arcak and Teel (2002), a proof of ISS for Lur'e-type systems is given, which is not applicable to systems with set-valued modeled friction laws. Next to the fact that the usually work on ISS considers continuous systems, they focus typically on the use of smooth ISS Lyapunov functions (see e.g. Arcak and Teel (2002), Sontag and Wang (1995) and Sontag (1989) to mention just a few). In case of extending the Popov criterion to the discontinuous systems as considered here, one has to adopt non-smooth (ISS) Lyapunov functions. The reason of non-smoothness is that the Lyapunov function contains a term consisting of an integral of the nonlinearity. Despite some recent attempts, see Cai and Teel (2005), Vu, Chatterjee, and Liberzon (2007) and Heemels, Weiland, and Juloski (2007), to bring ISS concepts to the realm of discontinuous and switched systems, none of these papers can be used in the present context.

Much experimental work is performed on the control of systems with collocation of actuation and friction, e.g. in the field of friction compensation for an industrial hydraulic robot (Lischinsky, Canudas-de-Wit, & Morel, 1999), a KUKA robot (Swevers et al., 2000), a robotic gripper (Johnson & Lorenz, 1992), etc. However, to the best of our knowledge, no experimental work is performed for stabilization of setpoints for systems with non-collocation of actuation and set-valued modeled friction. Here, we will apply the proposed output-feedback controller to an experimental rotor dynamic system, which represents a typical motion control example of a motor-load system with non-collocation of actuation and set-valued friction laws. Earlier work (Mihajlović et al., 2006) has shown that this system exhibits stick–slip limit cycling. The control proposed here will eliminate these limit cycles. Moreover, it will be shown that the circle criterion is not feasible for this system implying that the extension of the Popov criterion is indispensable within this context. The effectiveness of the designed output-feedback controller is shown in simulations and experiments.

The structure of this paper is as follows: We start with some notation in Section 2. In Section 3, we introduce models that include set-valued nonlinearities in their structure, representing a large class of mechanical motion systems with dry friction. The control designs are presented in Section 4, where we discuss the state-feedback control design with the generalization of the Popov criterion and the absolute ISS property, the observer design and the output-feedback control design. A rotor dynamic system is presented in Section 5 as an example of a mechanical system with non-collocated actuation and set-valued friction laws and the results of the application of the output-feedback control design are shown in simulations and experiments. We finish this paper with conclusions in Section 6.

2. Notations and definitions

A function $u : \mathbb{R}_+ \to \mathbb{R}^n$ is piecewise continuous, if on every bounded interval the function has only a finite number of points at which it is discontinuous. Without loss of generality we will assume that every piecewise continuous function u is right continuous, i.e. $\lim_{t\downarrow\tau} u(t) = u(\tau)$ for all $\tau \in \mathbb{R}_+$. With $\|\cdot\|$ we will denote the usual Euclidean norm for vectors in $\mathbb{R}^n$, and $\|\cdot\|_1$ denotes the 1-norm. A function $\gamma : \mathbb{R}_+ \to \mathbb{R}_+$ is of class $\mathcal{K}$ if it is continuous, strictly increasing and $\gamma(0) = 0$. It is of class $\mathcal{K}_\infty$ if, in addition, it is unbounded, i.e. $\gamma(s) \to \infty$ as $s \to \infty$. A function $\beta : \mathbb{R}_+ \times \mathbb{R}_+ \to \mathbb{R}_+$ is of class $\mathcal{KL}$ if, for each fixed $t \in \mathbb{R}_+$, the function $\beta(\cdot, t)$ is of class $\mathcal{K}$, and for each fixed $s \in \mathbb{R}_+$, the function $\beta(s, \cdot)$ is decreasing and tends to zero at infinity. $\lambda_{\min}(A)$, $\lambda_{max}(A)$ denote the minimal and maximal eigenvalue of the matrix A, respectively. A differential inclusion is given by an expression of the form

$$\dot{x}(t) \in F(x(t), e(t)), \quad (1)$$

where F is a set-valued mapping and $x \in \mathbb{R}^n$, $e \in \mathbb{R}^m$ represent the state and input, respectively. An absolutely continuous function x

is considered to be a strong solution of the differential inclusion (1) if (1) is satisfied almost everywhere. Let us define the graph of a set-valued function $f : \mathbb{R}^n \to \mathbb{R}^n$ by $\text{Graph}(f) = \{(x, y) \in \mathbb{R}^n \times \mathbb{R}^n \mid x \in \mathbb{R}^n, y \in f(x)\}$. A set $\mathcal{S}$ is a set of isolated points if for every point $a \in \mathcal{S}$ there exists an $\varepsilon > 0$ such that $[a - \varepsilon, a + \varepsilon] \cap \mathcal{S} = \{a\}$. The point a is an accumulation point of a set $\mathcal{S}$ if there exists a sequence $\{a_l\}$, $l \in \mathbb{N}$, with $a_l \in \mathcal{S}$ and $a_l \neq a$ for all $l \in \mathbb{N}$, such that $\lim_{l\to\infty} a_l = a$.

Definition 1 (*Sontag (1995)*). The system (1) is said to be input-to-state stable (ISS) if there exist a function β of class $\mathcal{KL}$ and a function γ of class $\mathcal{K}$ such that for each initial condition $x(0) = x_0$ and each piecewise continuous bounded input function e defined on $[0, \infty)$,

- all solutions x of the system (1) exist on $[0, \infty)$ and,
- all solutions satisfy

$$\|x(t)\| \le \beta(\|x_0\|, t) + \gamma(\sup_{\tau\in[0,t]} \|e(\tau)\|), \quad \forall t \ge 0. \tag{2}$$

The system is called globally asymptotically stable (GAS) if the above holds for $e = 0$.

Consider the following linear system

$$\begin{aligned} \dot{x} &= Ax + Gw \\ z &= Hx + Dw, \end{aligned} \tag{3}$$

with the state $x \in \mathbb{R}^n$, input and output $w, z \in \mathbb{R}^p$.

Definition 2. The system (3) or the quadruple (A, G, H, D) is said to be strictly passive if there exist an $\varepsilon > 0$ and a matrix $P = P^T > 0$ such that

$$\begin{bmatrix} A^\top P + PA + \varepsilon I & PG - H^\top \\ G^\top P - H & -D - D^\top \end{bmatrix} \le 0. \tag{4}$$

3. Mechanical motion systems with set-valued friction laws

A large class of mechanical motion systems with dry friction can be described by the following second-order form (Glocker, 2001):

$$M\ddot{q} + D\dot{q} + Kq = Su + T\lambda_T, \tag{5}$$

with the generalized coordinates $q \in \mathbb{R}^{n/2}$, the control input $u \in \mathbb{R}^m$, friction forces $\lambda_T \in \mathbb{R}^p$ and the mass, damping and stiffness matrices $M \in \mathbb{R}^{n/2\times n/2}$, $D \in \mathbb{R}^{n/2\times n/2}$ and $K \in \mathbb{R}^{n/2\times n/2}$, respectively. The matrices $S \in \mathbb{R}^{n/2\times m}$ and $T \in \mathbb{R}^{n/2\times p}$ represent the generalized force directions of the actuation and friction, respectively. We adopt the following set-valued friction law (cf. Glocker (2001)) for the ith frictional contact $\lambda_{T,i}$:

$$\begin{aligned} \lambda_{T,i} \in{}& -\mu_i\lambda_{N,i}\,\text{Sign}(T_i^\top\dot{q}) + F_{S,i}(T_i^\top\dot{q}) \\ =:{}& F_{f,i}(T_i^\top\dot{q}) \quad \text{for } i = 1, \dots, p. \end{aligned} \tag{6}$$

Herein, T_i represents the ith column of T and $T_i^\top\dot{q}$ is the sliding velocity in contact i. Note that the sliding velocity and the friction forces are aligned and, therefore, the friction laws are a function of $T_i^\top\dot{q}$. The first part in (6) reflects a set-valued Coulomb friction law with

$$\text{Sign}(y) \triangleq \begin{cases} \{-1\}, & y < 0 \\ [-1, 1] & y = 0 \\ \{1\}, & y > 0. \end{cases} \tag{7}$$

Moreover, μ_i and $\lambda_{N,i}$ are the Coulomb friction coefficient and the normal force in contact i, respectively. The second contribution to the friction law (6) is the smooth function $F_{S,i}(T_i^\top\dot{q})$, which models the velocity dependency of the friction. The equations (5) and (6) together constitute a differential inclusion which can be written in the following state-space form:

$$\dot{x} = Ax + Gw + Bu \tag{8a}$$

$$z = Hx \tag{8b}$$

$$y = Cx \tag{8c}$$

$$w \in -\varphi(z), \tag{8d}$$

where $x = [q^\top \ \ \dot{q}^\top]^\top \in \mathbb{R}^n$ is the system state, $w \in \mathbb{R}^p$ is the output, $z \in \mathbb{R}^p$, with $z = T^\top\dot{q}$, is the input of a set-valued nonlinearity φ, $u \in \mathbb{R}^m$ is the control input and $y \in \mathbb{R}^\kappa$ is the measured output. The matrices $A \in \mathbb{R}^{n\times n}$, $B \in \mathbb{R}^{n\times m}$, $G \in \mathbb{R}^{n\times p}$ and $H \in \mathbb{R}^{p\times n}$ are given by

$$A = \begin{bmatrix} 0 & I \\ -M^{-1}K & -M^{-1}D \end{bmatrix}, \qquad G = \begin{bmatrix} 0 \\ M^{-1}T \end{bmatrix}, \tag{9a}$$

$$B = \begin{bmatrix} 0 \\ M^{-1}S \end{bmatrix}, \qquad H = \begin{bmatrix} 0 & T^\top \end{bmatrix}, \tag{9b}$$

and $C \in \mathbb{R}^{\kappa\times n}$ is indicating the measured output. Finally, the nonlinearity $\varphi = \left[\varphi_i(z_i) \dots \varphi_p(z_p)\right]^\top$ is defined by

$$\varphi_i(z_i) = -F_{f,i}(z_i) \quad i = 1, \dots, p. \tag{10}$$

Note that if the image of T (respectively, G) is not contained in the image of S (respectively, B), then the actuation and the friction are non-collocated (at least partly) and direct friction compensation is impossible. The state-space equations (8) are in Lur'e-type form, which means that the system consists of a linear system (8a), (8b), (8c) with the set-valued nonlinearity (8d) in the feedback loop.

4. Control design for Lur'e-type systems

In this section, we design controllers for systems in the form (8) aiming at the stabilization of the origin $x = 0$. We first state the following assumptions on the properties of the set-valued nonlinearity $\varphi(z)$ in (8d).

Assumption 3. The set-valued nonlinearity $\varphi : \mathbb{R}^p \to \mathbb{R}^p$ satisfies

- $0 \in \varphi(0)$;
- φ is upper semicontinuous (see Aubin and Cellina (1984));
- φ is decomposed as $\varphi(z) = [\varphi_1(z_1), \dots, \varphi_p(z_p)]^\top$, $z = [z_1, \dots, z_p]^\top$ and $\varphi_i : \mathbb{R} \to \mathbb{R}$, for $i = 1, \dots, p$;
- φ_i, $i = 1, \dots, p$, are only set-valued on a countable set (of Lebesgue measure zero) of isolated points;
- for all $z_i \in \mathbb{R}$ the set $\varphi_i(z_i) \subseteq \mathbb{R}$, $i = 1, \dots, p$, is non-empty, convex, closed and bounded;
- each φ_i satisfies the $[0, \infty]$ sector condition in the sense that

$$z_i w_i \le 0 \quad \text{for all } w_i \in -\varphi_i(z_i) \text{ for } i = 1, \dots, p; \tag{11}$$

- there exist positive constants γ_1 and γ_2 such that for $w \in -\varphi(z)$ and for any $z \in \mathbb{R}^p$ it holds that

$$\|w\| \le \gamma_1\|z\| + \gamma_2. \tag{12}$$

The input functions $u(\cdot)$ are assumed to be in the space of piecewise continuous bounded functions from $[0, \infty)$ to $\mathbb{R}^m$, denoted by $\mathbb{PC}$. Clearly, the nonlinear function $(t, x) \mapsto Ax - G\varphi(Hx) + Bu(t)$ is upper semicontinuous on intervals, where u is continuous and attains non-empty, convex, closed and bounded set-values. From Aubin and Cellina (1984, p. 98) or Filippov (1988, Section 7), it follows that local existence of solutions is guaranteed given an initial state x_0 at initial time 0. Due to the growth condition (12), finite escape times are prevented and thus any solution to (8) is globally defined on $[0, \infty)$. Hence, solutions $x(\cdot)$ and also $z(\cdot) = Hx(\cdot)$ are absolutely continuous functions. Note that $0 \in \varphi(0)$ implies that the origin $x = 0$ is an equilibrium (which may belong to an equilibrium set) of the open-loop system (8) for input $u = 0$.

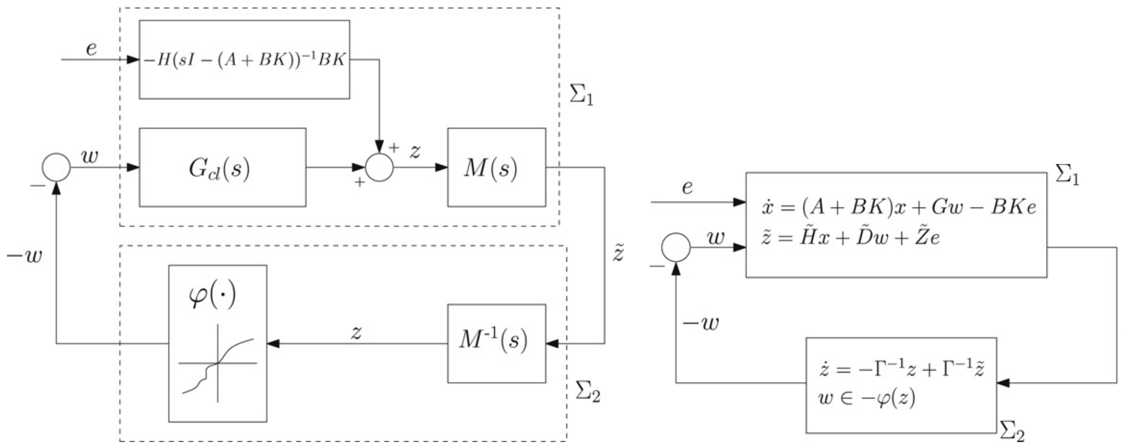

(a) Cascade representation of system (14) using the dynamic multiplier (16). (b) Closed-loop system (17) after transformation with dynamic multiplier (16).

Fig. 1. Block diagrams of the closed-loop system (17).

4.1. State-feedback control

In order to make the origin $x = 0$ of system (8) a unique isolated equilibrium point, that is globally asymptotically stable, we propose a linear static state-feedback law (assuming $C = I$ and, therefore, $y = x$ for this case) where we take the measurement error e into account, which is piecewise continuous and bounded:

$$u = K(x - e). \tag{13}$$

Here, $K \in \mathbb{R}^{m\times n}$ is the control gain matrix. Consequently, the resulting closed-loop system is described by the following differential inclusion:

$$\begin{aligned}\dot{x} &= (A + BK)x + Gw - BKe\\ z &= Hx\end{aligned} \tag{14a}$$

$$w \in -\varphi(z). \tag{14b}$$

The transfer function $G_{cl}(s)$ from the input w to the output z of system (14) is given by

$$G_{cl}(s) = H(sI - (A + BK))^{-1}G, \quad s \in \mathbb{C}. \tag{15}$$

The intended control goal here is to render the closed-loop system (14) "absolutely ISS" with respect to e, as formalized below, by means of a proper choice of the control gain K.

Definition 4. We call a system (14) absolutely ISS with respect to input e, if the system (14) is ISS with respect to input e, as in Definition 1, for any φ satisfying Assumption 3.

To obtain sufficient conditions to guarantee that system (14) is absolutely ISS, we use, as in Khalil (2002) for smooth systems, a so-called dynamic multiplier with transfer function $M(s)$ given by

$$M(s) = I + \Gamma s, \quad s \in \mathbb{C}, \tag{16}$$

where $\Gamma = \text{diag}(\eta_1, \dots \eta_p) \in \mathbb{R}^{p\times p}$, with $\eta_i > 0$ for $i = 1, \dots, p$. The inverse of $M(s)$ will be chosen to be passive, because (as we will explain later) the multiplication of the set-valued nonlinearity in (14) with the inverse of the dynamic multiplier must yield a passive system. A cascade that represents system (14) together with the multiplier $M(s)$ is shown in Fig. 1. Using the dynamic multiplier $M(s)$ we aim to transform the original system into a feedback interconnection of two passive systems (with the perturbation input e), as is done in Khalil (2002) and Arcak et al. (2003) for systems with Lipschitz continuous nonlinearities.

In state-space formulation, the interconnected system Σ_1, Σ_2 takes the following form:

$$\Sigma_1 = \begin{cases}\dot{x} = (A + BK)x + Gw - BKe(t)\\ \tilde{z} = \tilde{H}x + \tilde{D}w + \tilde{Z}e(t)\end{cases} \tag{17a}$$

$$\Sigma_2 = \begin{cases}\dot{z} = -\Gamma^{-1}z + \Gamma^{-1}\tilde{z}\\ w \in -\varphi(z).\end{cases} \tag{17b}$$

See also Fig. 1. Herein, $\tilde{z} \in \mathbb{R}^p$ and the matrices $\tilde{H} \in \mathbb{R}^{p\times n}$, $\tilde{D} \in \mathbb{R}^{p\times p}$ and $\tilde{Z} \in \mathbb{R}^{p\times n}$ can be derived from the fact that $\tilde{z} = z + \Gamma\dot{z}$ (due to the choice of the multiplier $M(s)$ as in (16)) and hence,

$$\begin{aligned}&\tilde{H} = H + \Gamma H(A + BK),\\ &\tilde{D} = \Gamma HG, \qquad \tilde{Z} = -\Gamma HBK.\end{aligned} \tag{18}$$

The following theorem states sufficient conditions under which system (14) is ISS with respect to input e for any $\varphi \in [0, \infty]$, i.e. the system (14) is absolutely ISS.

Theorem 4.1. *Consider system (14) and suppose there exists a diagonal matrix $\Gamma = \text{diag}(\eta_1, \dots, \eta_p) \in \mathbb{R}^{p\times p}$ with $\eta_i > 0$, $i = 1, \dots, p$, such that $(A + BK, G, \tilde{H}, \tilde{D})$ with $\tilde{H}$ and $\tilde{D}$ as in (18) is strictly passive. Then system (14) is absolutely ISS with respect to input e for any φ satisfying Assumption 3.*

The proof of Theorem 4.1 is given in Appendix A. We also note that in (Yakubovich, Leonov, & Gelig, 2004), frequency-domain conditions (including Popov-type conditions) guaranteeing a property close to GAS are stated for Lur'e-type systems with discontinuous nonlinearities. Here, we provide a Popov-like criterion for systems with set-valued nonlinearities that guarantees ISS with respect to input e.
An advantage of achieving absolute ISS is, firstly, the robustness to uncertainties in the nonlinearity φ in the feedback loop and, secondly, the robustness with respect to input e. Note that the ISS gain is independent of the exact form of the nonlinearity φ. In case of mechanical motion systems as in (5) and (6), this means that we have robustness with respect to uncertainties in the friction model. Note that if the input e is zero, the origin $x = 0$ of system (14) is absolutely stable under the conditions of Theorem 4.1.

4.2. Observer design

Following (Doris et al., 2008), we propose the following observer for the system (8)

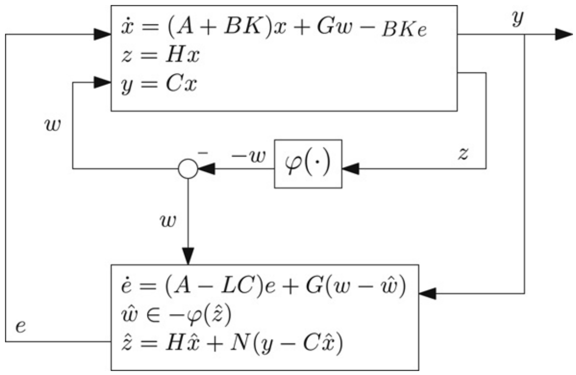

Fig. 2. Combination of the observer design and the controller design.

$$\dot{\hat{x}} = (A - LC)\hat{x} + G\hat{w} + Bu + Ly \tag{19a}$$

$$\hat{w} \in -\varphi(\hat{z}) \tag{19b}$$

$$\hat{z} = (H - NC)\hat{x} + Ny \tag{19c}$$

$$\hat{y} = C\hat{x} \tag{19d}$$

with the observer gains $N \in \mathbb{R}^{p\times\kappa}$ and $L \in \mathbb{R}^{n\times\kappa}$.

At this point, we state an additional assumption on the set-valued nonlinearity $\varphi(\cdot)$ of system (8):

Assumption 5. The set-valued nonlinearity $\varphi : \mathbb{R}^p \to \mathbb{R}^p$ is such that φ is monotone, i.e. for all $z_1 \in \mathbb{R}^p$ and $z_2 \in \mathbb{R}^p$ with $w_1 \in \varphi(z_1)$ and $w_2 \in \varphi(z_2)$, it holds that $\langle w_1 - w_2, z_1 - z_2\rangle \geq 0$, where $\langle\cdot,\cdot\rangle$ denotes the inner product in $\mathbb{R}^p$.

Since the right-hand side of (19a) is again upper semicontinuous in (t, x) due to continuity of y and piecewise continuity of u, using Assumptions 3 and 5 on φ it can be shown that there exist global solutions of (19) (Aubin & Cellina, 1984; Filippov, 1988). Also, the solutions $\hat{x}$ and $\hat{w}$ are unique a.e. and knowing that both the plant and the observer have global solutions, the dynamics for the observer error $e := x - \hat{x}$ is given by

$$\dot{e} = (A - LC)e + G(w - \hat{w}) \tag{20a}$$

$$w \in -\varphi(Hx) \tag{20b}$$

$$\hat{w} \in -\varphi(H\hat{x} + N(y(t) - C\hat{x})). \tag{20c}$$

The problem of the observer design is finding the gains L and N such that all solutions to the observer error dynamics converge exponentially to the origin, which implies that $\lim_{t\to\infty} |\hat{x}(t) - x(t)| = 0$.

Theorem 4.2 (*Doris et al., 2008*). *Consider system (8) and the observer (19) with $(A - LC, G, H - NC, 0)$ strictly passive and the matrix G being of full column rank. Then, the point $e = 0$ is a globally exponentially stable equilibrium point of the observer error dynamics (20) for any $\varphi(\cdot)$ satisfying Assumptions 3 and 5.*

4.3. Output-feedback control

In this section, an observer-based output-feedback controller is presented, where we use the observer design, presented in the previous section, to estimate the system state. Next, the estimated state $\hat{x}$ is fed back to the system (8) with $u = K\hat{x} = K(x - e)$ as in (13), where e now represents the estimation error. Application of the observer-based output-feedback controller results in an interconnection of system (14) and system (20), which is depicted in Fig. 2. We aim to prove global asymptotic stability (GAS) of the equilibrium $(x, e) = (0, 0)$ of the interconnected system (14), (20).

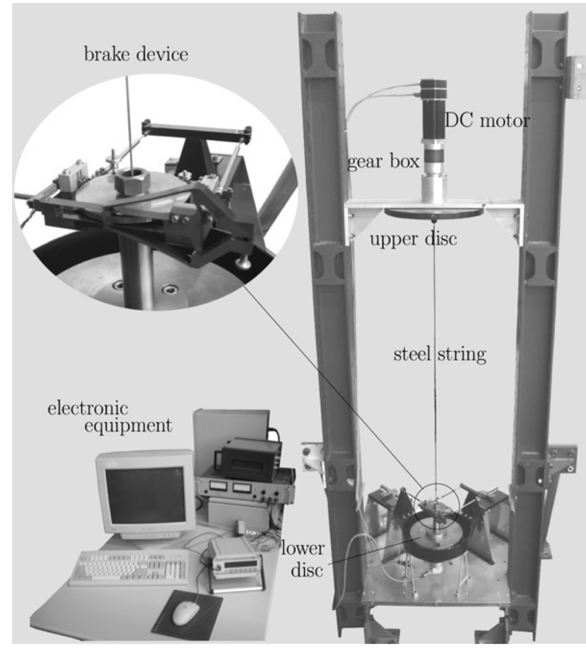

Fig. 3. Photo of the rotor dynamic setup.

Theorem 4.3. *Consider system (14) and observer (19). Suppose there exists a matrix $\Gamma = diag(\eta_1, \ldots, \eta_p) \in \mathbb{R}^{p\times p}$ with $\eta_i > 0$, $i = 1, \ldots, p$, such that $(A + BK, G, \tilde{H}, \tilde{D})$ is strictly passive with $\tilde{G}$ and $\tilde{H}$ as in (18). Moreover, suppose, $(A - LC, G, H - NC, 0)$ is strictly passive and G being full column rank. Then, $(x, e) = (0, 0)$ is a globally asymptotically stable equilibrium point of the interconnected system (14), (20) for any $\varphi(\cdot)$ satisfying Assumptions 3 and 5.*

Proof. According to Theorem 4.1, under the hypotheses of the current theorem, system (14) is ISS with respect to the observer error $e(t)$. Moreover, according to Theorem 4.2, the observer error dynamics are globally exponentially stable. Using the proof of Lemma 4.7 in (Khalil, 2002), we can conclude that $(x, e) = (0, 0)$ is a globally asymptotically stable equilibrium point of system (14), (20). Note that Lemma 4.7 in (Khalil, 2002) is given for locally Lipschitzian systems. However, the proof is given on a trajectory level and, therefore, it can also be applied to differential inclusions. □

5. Application to a rotor dynamic system with friction

5.1. Experimental setup and modeling

The experimental setup consists of an upper disc actuated by a drive part (consisting of a power amplifier, DC-motor and a gear box), a steel string, a lower disc and a brake device, see Fig. 3. The actuator input voltage of the drive part is limited to the range $[-5V, 5V]$. The upper disc is connected to the lower disc by a steel string, which is a low-stiffness connection between the discs. A brake disc is connected to the lower disc and a brake device exerts a normal force to it. Oil is supplied to create an oil layer between the disc and the brake device, resulting in a friction characteristic with a Stribeck effect (Olsson et al., 1998) (i.e. with a so-called negative damping characteristic). Two incremental encoders are used to measure the angular positions of the lower and the upper discs. The configuration of the experimental setup can be recognized in the structure of drilling systems and other rotor dynamic motion systems.

We define u as the input voltage to the drive part. The system has two degrees of freedom: the angular displacements of the

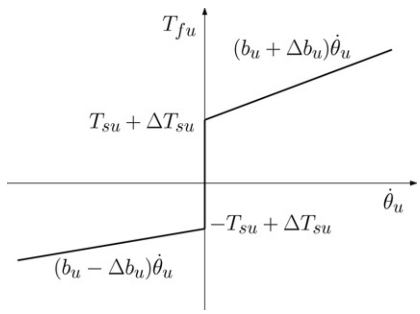

Fig. 4. Upper friction model T_{fu}.

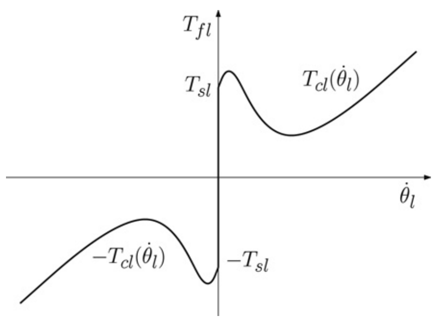

Fig. 5. Lower friction model T_{fl}.

upper and lower discs, θ_u and θ_l, respectively. The equations of motion for the upper disc and the lower disc are given by

$$J_u\ddot{\theta}_u + k_\theta(\theta_u - \theta_l) + b(\dot{\theta}_u - \dot{\theta}_l) + T_{fu}(\dot{\theta}_u) - k_m u = 0 \quad (21)$$
$$J_l\ddot{\theta}_l - k_\theta(\theta_u - \theta_l) - b(\dot{\theta}_u - \dot{\theta}_l) + T_{fl}(\dot{\theta}_l) = 0.$$

Set-valued force laws are needed to model the friction acting on the upper and lower disc to account for the pronounced sticking effect in both characteristics. The friction torque acting on the upper disc is caused by the electromagnetic field in the drive part and the bearings that support the disc and is modeled by T_{fu}, see Fig. 4:

$$T_{fu}(\dot{\theta}_u) \in \begin{cases} T_{cu}(\dot{\theta}_u)\mathrm{sgn}(\dot{\theta}_u) & \text{for } \dot{\theta}_u \neq 0 \\ [-T_{su} + \Delta T_{su}, \\ \quad T_{su} + \Delta T_{su}] & \text{for } \dot{\theta}_u = 0, \end{cases} \quad (22)$$

$$T_{cu}(\dot{\theta}_u) = T_{su} + \Delta T_{su}\mathrm{sgn}(\dot{\theta}_u) + b_u|\dot{\theta}_u| + \Delta b_u\dot{\theta}_u. \quad (23)$$

The friction torque T_{fl}, see Fig. 5, is caused by bearings that support the lower disc and, mainly, by the brake device and is represented by

$$T_{fl}(\dot{\theta}_l) \in \begin{cases} T_{cl}(\dot{\theta}_l)\mathrm{sgn}(\dot{\theta}_l) & \text{for } \dot{\theta}_l \neq 0 \\ [-T_{sl}, T_{sl}] & \text{for } \dot{\theta}_l = 0, \end{cases} \quad (24)$$

$$T_{cl}(\dot{\theta}_l) = T_{cl} + (T_{sl} - T_{cl})\mathrm{e}^{-\left|\frac{\dot{\theta}_l}{\omega_{sl}}\right|^{\delta_{sl}}} + b_l|\dot{\theta}_l|. \quad (25)$$

We define the state vector x as

$$x = \begin{bmatrix} x_1 \\ x_2 \\ x_3 \end{bmatrix} = \begin{bmatrix} \alpha \\ \omega_u \\ \omega_l \end{bmatrix} = \begin{bmatrix} \theta_u - \theta_l \\ \dot{\theta}_u \\ \dot{\theta}_l \end{bmatrix}. \quad (26)$$

Note that the state $x_1 = \alpha = \theta_u - \theta_l$ represents the relative angular displacement of the lower disc with respect to the upper disc, which can be obtained via the encoder measurements of θ_u and θ_l ($y = x_1$). The desired solution for the rotor dynamic system is a constant (and identical) velocity for both discs, which corresponds to an equilibrium (note that in drilling systems such constant velocity solution corresponds to nominal operating conditions). The state-space equations of the rotor dynamic system in Lur'e-type form are given by (8), with state $x \in \mathbb{R}^3$, $w, z \in \mathbb{R}^2$, input $u \in \mathbb{R}$, measured output $y \in \mathbb{R}$, and $\varphi(z) = [\varphi_1(z_1) \quad \varphi_2(z_2)]^\top = [T_{fu}(z_1) \quad T_{fl}(z_2)]^\top$ with $\varphi_i : \mathbb{R} \to \mathbb{R}$ for $i = 1, 2$. The matrices and the nonlinearity $\varphi(z)$ in (8) are given by

Table 1
Estimated parameters.

Parameter	Value	Unit
k_m	4.3228	[Nm/V]
J_u	0.4765	[kg m^2]
T_{su}	0.37975	[N m]
ΔT_{su}	−0.00575	[N m]
b_u	2.4245	[kg m^2/rad s]
Δb_u	−0.0084	[kg m^2/rad s]
k_θ	0.075	[N m/rad]
b	0	[kg m^2/rad s]
J_l	0.035	[kg m^2]
T_{sl}	0.26	[N m]
T_{cl}	0.05	[N m]
ω_{sl}	2.2	[rad/s]
δ_{sl}	1.5	[–]
b_l	0.009	[kg m^2/rad s]

$$A = \begin{bmatrix} 0 & 1 & -1 \\ -\frac{k_\theta}{J_u} & -b & b \\ \frac{k_\theta}{J_l} & b & -b \end{bmatrix}, \qquad B = \begin{bmatrix} 0 \\ \frac{k_m}{J_u} \\ 0 \end{bmatrix}, \quad (27)$$

$$G = \begin{bmatrix} 0 & 0 \\ \frac{1}{J_u} & 0 \\ 0 & \frac{1}{J_l} \end{bmatrix}, \qquad H = \begin{bmatrix} 0 & 1 & 0 \\ 0 & 0 & 1 \end{bmatrix}, \qquad C^\top = \begin{bmatrix} 1 \\ 0 \\ 0 \end{bmatrix}, \quad (28)$$

$$\varphi(z) = \begin{bmatrix} T_{fu}(z_1) \\ T_{fl}(z_2) \end{bmatrix}. \quad (29)$$

The parameters of the rotor dynamic model (8), (27), (28), (29) are estimated by dedicated parameter identification experiments, see Table 1, following a similar procedure as described in Mihajlović et al. (2006), and are validated by comparing the steady-state solutions of the simulations with those of the experiments.

For varying constant inputs u_c (i.e. $u = u_c$ in (8)), we observe several bifurcations in simulations and experiments. Different (co-existing) steady-state solutions of the rotor dynamic system as result of the simulations and experiments, are depicted in a bifurcation diagram in Fig. 6 for constant input voltages u_c, which is the bifurcation parameter. For the case where the steady-state response is a periodic solution (stick–slip limit cycle), we plot the maximum and minimum value of the state variable ω_l (velocity of the lower disc) in the bifurcation diagram. For the region with constant input voltages up to approximately $u_c = 2.7$ V, we observe only stable limit cycles. Fig. 7 shows such a limit cycle response for $u_c = 2.7$ V. In the region from approximately 2.7 to 4.5 V, two stable steady-state solutions co-exist: an equilibrium point or a stick–slip limit cycle, depending on the initial conditions. For constant input voltages higher than 4.5 V, only a stable equilibrium point occurs. The reader is referred to Mihajlović et al. (2006) for an extensive analysis of the dynamic behavior of the rotor dynamic system including the discussion of the bifurcations involved. As we remarked earlier, the equilibria of the rotor dynamic system correspond to both discs rotating with the same constant velocity, which are the desired operating conditions. As such, the control goal is to stabilize the unstable

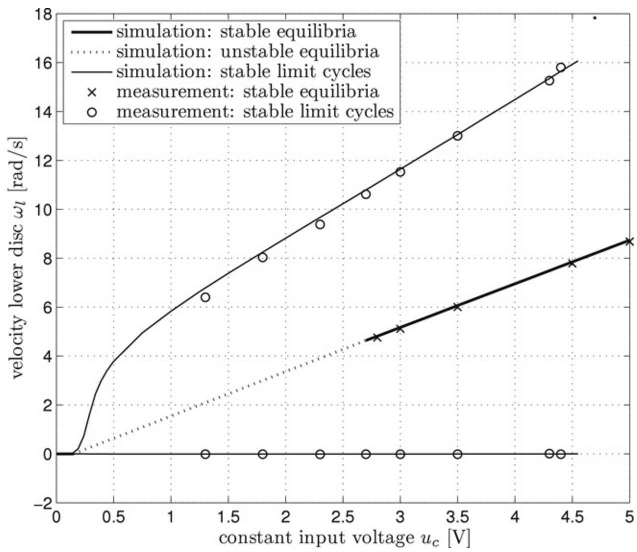

Fig. 6. Bifurcation diagram for the open-loop rotor dynamic system.

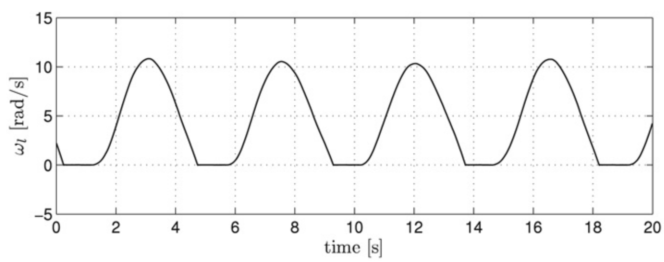

Fig. 7. Experimental limit cycle response of the rotor dynamic system for $u_c = 2.7$ V.

equilibria up to $u_c = 2.7$ V and to eliminate the limit cycles up to $u_c = 4.5$ V.

5.2. Output-feedback controller

One could opt to design an output-feedback controller by using the circle criterion, instead of the more involved Popov-criterion-inspired approach with the dynamic multiplier $M(s)$. However, the control design based on the circle criterion is not feasible for the rotor dynamic system (8) according the presented feasibility conditions in Arcak and Kokotović (2001). In order to satisfy the feasibility conditions in Arcak and Kokotović (2001), the damping coefficient b should satisfy $\{b > \min \frac{\partial}{\partial \omega_l} T_{fl}(\omega_l) | \omega_l > 0\}$. This would imply that the negative damping in the friction model T_{fl}, which is, basically, the cause of the friction-induced stick–slip vibrations is dominated by such viscous damping b in the string. However, the damping coefficient b reflects only material damping in the string which is generally very low and will not satisfy the above condition ($b = 0$, see Table 1). As many mechanical motion systems consist of inertias coupled by a low-damping connection, there exists a large class of systems for which a circle-criterion based control design is not feasible. For these systems, the output-feedback control design presented in Section 4.3 can be a solution since the use of the dynamic multiplier relaxes the circle-criterion conditions. The control strategy presented in Section 4.3 is applied to the rotor dynamic system (8) and the output-feedback control law is given by

$$u = u_c + u_{\text{comp}} + K(\hat{x} - x_{eq}), \tag{30}$$

with $x_{eq} = [\alpha_{eq}\ \ \omega_{eq}\ \ \omega_{eq}]^\top$ the desired equilibrium of the rotor dynamic system (8), the control gain $K \in \mathbb{R}^{1\times 3}$ and

$$u_{\text{comp}} = \frac{1}{k_m}(T_{fu}(\hat{x}_2) - b_u \hat{x}_2). \tag{31}$$

The part u_{comp} of the control law compensates partly the friction acting at the upper disc of the rotor dynamic system. The 'effective' friction after compensation acting at the upper disc is purely viscous. Note that such a friction compensation can not be employed to compensate for the friction at the lower disc (which is responsible for the stick–slip limit cycling), due to the non-collocation of actuation and friction. We can easily transform the closed-loop rotor dynamic system (8), (30) to a system in Lur'e-type form with the origin as equilibrium by choosing, for example, the new state $\xi = x - x_{eq}$. For the sake of brevity, we will omit this transformation here (see Doris (2007) for more details). Assumption 5 requires that the set-valued nonlinearity φ is monotone. If we consider the friction model T_{fl}, see Fig. 5, which is contained in φ, then it is clear that T_{fl} is not monotone. We will render φ monotone by applying a loop transformation, which will add 'viscous' damping to T_{fl} and subtract it from the linear part of (8), see Doris (2007). The following feedback and observer gains satisfy Theorem 4.3:

$$K^\top = \begin{bmatrix} 15.9 \\ 1.57 \\ 27.6 \end{bmatrix}, \qquad L = \begin{bmatrix} 195 \\ -312 \\ -9080 \end{bmatrix}, \qquad N = \begin{bmatrix} -2.22 \\ -37.8 \end{bmatrix}, \tag{32}$$

with the multiplier matrix $\Gamma = 10I$. A solution for P that satisfies the strict passivity condition for $(A + BK, G, \tilde{H}, \tilde{D})$ is

$$P = \begin{bmatrix} 3.639 & 0.431 & 6.382 \\ 0.431 & 0.070 & 0.740 \\ 6.382 & 0.740 & 11.627 \end{bmatrix}. \tag{33}$$

The above results are obtained by a linear matrix inequality (LMI) solving routine within the program MATLAB.

5.3. Simulations and experiments

The presented output-feedback controller is applied to the rotor dynamic system to stabilize the equilibria of the rotor dynamic setup for a large range of constant inputs. We show the experimental closed-loop transient response for the constant input voltage $u_c = 2.5$ V and $u_c = 4.0$ V, respectively, in Fig. 8. The only stable open-loop solution for $u_c = 2.5$ V is a stick–slip limit cycle, see Fig. 6. For an input of $u_c = 4.0$ V, two stable open-loop solutions exist: an equilibrium and a stick–slip limit cycle. The output-feedback controller is switched on at $t = 5$ s for $u_c = 2.5$ V and the closed-loop system converges to the equilibrium state ($\omega_{eq} = 4.40$ rad/s). Also for $u_c = 4.0$ V, the closed-loop system converges to the equilibrium state ($\omega_{eq} = 7.06$ rad/s) where the initial open-loop solution is a stick–slip limit cycle. Both experimental and model-based bifurcation diagrams for the closed-loop rotor dynamic system are depicted in Fig. 9. The simulated bifurcation diagram shows that for all constant u_c the desired equilibrium is globally asymptotically stabilized. In experiments, the output-feedback controller is able to eliminate the stable limit cycles and to stabilize the unstable equilibria for a large range of constant inputs u_c. However, for a small range of low voltages, the output-feedback controller can not stabilize the equilibria of the experimental rotor dynamic setup. The remaining closed-loop limit cycles up to $u_c = 1.5$ V differ from the open-loop limit cycles. A cause for this lack of stability of the equilibria at these low input voltages may be some unmodeled position-dependent friction acting on the lower disc.